Imaging the seizure onset zone with stereo-electroencephalography.

Olivier David, Thomas Blauwblomme, Anne-Sophie Job, Stéphan Chabardès, Dominique M. Hoffmann, Lorella Minotti, Philippe Kahane

Imaging the seizure onset zone with stereo-electroencephalography

Olivier David [a,b,c,*], Thomas Blauwblomme [d], Anne-Sophie Job [e], Stéphan Chabardès [a,b,f], Dominique Hoffmann [f], Lorella Minotti [b,e], Philippe Kahane [b,e,g]

[a] Fonctions Cérébrales et Neuromodulation, Université Joseph Fourier, Grenoble, France

[b] Inserm, U836, Grenoble Institut des Neurosciences, Grenoble, France

[c] Clinique Universitaire de Neuroradiologie et IRM, Centre Hospitalier Universitaire, Grenoble, France

[d] Service de Neurochirurgie Pédiatrique, Hôpital Necker, Université Paris Descartes, Sorbonne Paris Cité, Paris, France

[e] Laboratoire de Neurophysiopathologie de l'Epilepsie, Centre Hospitalier Universitaire, Grenoble, France

[f] Clinique Universitaire de Neurochirurgie, Pôle Tête et Cou, Centre Hospitalier Universitaire, Grenoble, France

[g] IDEE, Centre Hospitalier Universitaire, Lyon, France

* Corresponding author:
Olivier David, PhD
Grenoble Institut des Neurosciences
Chemin Fortuné Ferrini – Bât EJ Safra – CHU
38700 La Tronche, France
Email: odavid@ujf-grenoble.fr
Tel: +33 4 56 52 05 86
Fax: +33 4 56 52 05 98

Running title: Seizure onset zone imaging

Total number of words in the text: 5841

Revision of BRAIN-2011-00826.R1

August 2011

ABSTRACT

Stereo-electroencephalography is used to localise the seizure onset zone and connected neuronal networks in surgical candidates suffering from intractable focal epilepsy. The concept of epileptogenicity index has been proposed recently to represent the likelihood of various regions being part of the seizure onset zone. It quantifies low-voltage fast activity, the electrophysiological signature of seizure onset usually assessed visually by neurologists. Here, we revisit epileptogenicity in light of neuroimaging tools such as those provided in the Statistical Parametric Mapping software. Our goal is to propose a robust approach, allowing easy exploration of patients' brains in time and space. The procedure is based upon statistical parametric mapping, which is an established framework for comparing multi-dimensional image data that allows one to correct for inherent multiple comparisons. Statistics can also be performed at the group level, between seizures in the same patient, or between patients suffering from the same type of epilepsy using normalisation of brains to a common anatomic atlas. Results are obtained from three case studies (insular reflex epilepsy, cryptogenic frontal epilepsy, lesional occipital epilepsy) where tailored resection was performed, and from a group of 10 patients suffering from mesial temporal lobe epilepsy. They illustrate the basics of the technique and demonstrate its very good reproducibility and specificity. Most importantly, the proposed approach to the quantification of the seizure onset zone allows one to summarize complex signals in terms of a time-series of statistical parametric maps that can support clinical decisions. Quantitative neuroimaging of stereo-electroencephalographic features of seizures might thus help to provide better presurgical assessment of patients undergoing resective surgery.

Keywords: intracranial electroencephalogram, EEG discharges, signal analysis, neuroimaging, mesial temporal lobe epilepsy

I INTRODUCTION

The primary aim of epilepsy surgery is to remove the epileptogenic zone - “the minimum amount of cortex that must be resected (inactivated or completely disconnected) to produce seizure freedom" (Rosenow and Luders, 2001). The identification of the cortical area to be removed is a difficult process. In 25-50% of the cases, it requires intracranial electrodes, either at the surface of the brain (grids, strips) or deep inside the brain (stereo-electroencephalography, SEEG) (Spencer *et al.* , 2008). Such intracranial EEG (IEEG) recordings are used to delineate the cortical areas where seizures start and rapidly propagate, based on visual inspection of IEEG signals. For a long time, emphasis has been put on the identification of high-frequency oscillations (HFO) in the beta and gamma frequency ranges, often referred to as (low voltage) fast discharges, which could be a specific electrophysiological signature of the epileptogenic brain tissue (Allen *et al.* , 1992, Bancaud *et al.* , 1970, Fisher *et al.* , 1992, Wendling *et al.* , 2003, Worrell *et al.* , 2004). Recent improvements in acquisition technology have revealed neural activity at frequencies as fast as 400 Hz at seizure onset (Jirsch *et al.* , 2006). However, not all operated patients are cured following surgery, even when using intracranial information (Tellez-Zenteno *et al.* , 2005), which reflects the fact that there is still no established electrophysiological criteria to unequivocally identify the brain areas which must be surgically targeted.

An important step towards the quantification of the likelihood of regions being involved in seizure onset, or “epileptogenicity”, has recently been made by introducing the notion of *epileptogenicity index* (EI) (Bartolomei *et al.* , 2008). This index has been applied to SEEG signals to perform quantified studies of different

types of seizures: mesial temporal and temporosylvian (Bartolomei *et al.* , 2008, Bartolomei *et al.* , 2010), parietal (Bartolomei *et al.* , 2011), hyperkinetic of temporal origin (Vaugier *et al.* , 2009), or associated with cortical dysplasias and neurodevelopmental tumours (Aubert *et al.* , 2009). In these studies, the EI was often found to be high in regions suspected from aetiology to correspond to the seizure onset zone (SOZ). Furthermore, the number of epileptogenic regions, *i.e.* with a high EI, significantly correlated with epilepsy duration, but only in some of epilepsies investigated so far. Current results based on EI are thus very interesting, particularly to better classify epilepsies and to improve scoring of seizures recorded with SEEG during presurgical evaluations.

In general, any EI is based on the quantification, by the means of summary statistics, of specific SEEG features that define electrophysiological signatures of epileptogenic circuitry. In focal seizures for instance, it is now commonly accepted that regions showing transient fast (> 15 Hz) oscillations, *i.e.* rapid discharges, are likely to be related to the SOZ (Bancaud *et al.* , 1970), all the more when they occur at an early stage during seizure development. For instance, Worrell and collaborators have shown that power between 60 and 100 Hz increases after seizure onset in suspected regions being part of the SOZ (Worrell *et al.* , 2004). In the implementation of the EI proposed by Bartolomei et al. (2008), spectral (< 97 Hz) and temporal information are mixed together in the summary statistics, which basically quantify, for each electrode, the power of high frequencies normalised by the power of low frequencies (assuming a flattening of SEEG signals during rapid discharges) and weighted by the latency of appearance of rapid discharges. It is also suspected that HFO (> 100 Hz) are involved during focal seizures, as shown in humans (Jirsch *et al.* , 2006, Gnatkovsky

et al. , 2011) and animals (Grenier *et al.* , 2003). Recently, using the integral of SEEG power as a measure of seizure onset, the Milan group also found that HFO at seizure onset might be preceded by low frequency oscillations (< 20 Hz) (Gnatkovsky *et al.* , 2011). Empirically however, the specificity of defining the SOZ on the basis of fast oscillations has been demonstrated by showing that the resection of regions showing early fast activity predicts surgical prognosis (Alarcon *et al.* , 1995).

Although the implementation of EI by Bartolomei et al. (2008) and by Gnatkovsky et al. (2011) is very efficient, we here propose significant modifications to the methodology, while keeping its philosophy intact. In particular, we adopt a neuroimaging approach, assuming that many SEEG recording sites can be obtained, in order to generate statistical parametric maps (SPM) of EI. Our goal is to propose a comprehensive approach to EI that allows to proceed to standard statistical testing, either at the patient level or at the group level. Briefly, methodology aims at identifying brain areas whose high frequency activity is significantly greater than baseline using standard techniques from imaging time-series analysis. This involves a simple categorical comparison (using T-tests) between mean activity at baseline and mean activity over short windows (*e.g.* 4 s) at various times (*e.g.* from 0 s up to 20 s) after seizure onset. The significance of these differences is evaluated in relation to the variability of fluctuations within each time segment. The data features we choose to compare are the fluctuations in power in a frequency band of interest (e.g. 60-100 Hz).

Efficient visualisation of EI results allowed by our neuroimaging framework is also important for clinical practice, with potential multimodal comparisons, *e.g.* with

functional magnetic resonance imaging (fMRI) or positron emission tomography (PET). In this technical report, we will use a well-documented case study of insular epilepsy (Blauwblomme *et al.* , In press) to illustrate the different steps of our procedure. We will also demonstrate its clinical utility in two other patients suffering from cryptogenic frontal epilepsy and lesional occipital epilepsy and in whom tailored resection of the SOZ was performed. Finally, a group analysis of 10 patients suffering from mesial temporal lobe epilepsy (MTLE) will show the potential of this type of approach.

II MATERIALS AND METHODS

II.1 Clinical procedure and data acquisition

Patients included in this study have been selected for resective surgery and have undergone standard presurgical evaluations (high resolution MRI, video-EEG monitoring, neuropsychological testing). In addition, SEEG recordings were judged necessary before surgery to better delineate the brain areas to be resected. They were conducted according to the methodology described in (Kahane et al., 2004).

Patients were fully informed of the clinical procedure and gave their consent before being implanted. Eleven to fifteen semirigid intracerebral electrodes were implanted per patient, in various cortical areas depending on the suspected origin of seizures. Each electrode was 0.8 mm in diameter and included 5, 10, 15 or 18 leads 2 mm in length, 1.5 mm apart (Dixi Microtechniques, Besançon, France), depending on the target region. A preoperative stereotaxic MRI and a stereotaxic teleradiography

matched with Talairach and Tournoux's stereotaxic atlas (Talairach and Tournoux, 1988) were used to assess anatomical targets. Implantation of the electrodes was performed in the same stereotaxic conditions, with the help of a computer-driven robot (Neuromate, ISS). The location of the electrode contacts was subsequently reported on a stereotaxic scheme for each patient and defined by their coordinates in relation to the anterior commissure / posterior commissure plane. They were expressed in the coordinate system of Montreal Neurological Institute (MNI) to allow group analyses.

SEEG recordings were performed using an audio-video-EEG monitoring system (Micromed, Treviso, Italy) that allowed to simultaneously record up to 256 contacts, so that a large range of mesial and cortical areas was sampled. Sampling rate was either 256 or 512 Hz, with an acquisition band-pass filter between 0.1 and 90 Hz or between 0.1 and 200 Hz respectively, depending on amplifier capacities at the date of recordings. Data were acquired using a referential montage with reference electrode chosen in the white matter. For data analysis, we used a bipolar montage between adjacent leads of the same electrode to improve sensitivity to local oscillations. Coordinates of virtual bipolar electrodes that are used to construct images were chosen to be at equal distance of two successive leads.

II.2 Patients

To illustrate the potential of the approach for single subject studies, we selected three patients who were seizure-free following tailored resection of the SOZ. First to explain and validate the methodology, we chose a fully documented case report of insular reflex epilepsy to strawberry syrup consumption (Blauwblomme *et al.* , In

press). In this patient (Patient A), two complete seizures were recorded in SEEG using 168 electrode contacts, equivalent to 100 adjacent bipolar recordings, implanted in the right hemisphere. SEEG signals showed the involvement of a fronto-parieto-insulo-hippocampal epileptogenic network. They are reanalysed here using the EI approach. This patient was cured after resection of the middle short gyrus of the right insula that was suspected to be the SOZ from multimodal comparison between semiology, SEEG and fMRI (Blauwblomme *et al.* , In press).

Second, to further demonstrate the clinical utility of our procedure, we selected two other cases (Patient B and Patient C) in whom SOZ identification was difficult but facilitated by the proposed methodology. Patient B was suffering from cryptogenic frontal epilepsy with hypermotor seizures. SEEG recordings (91 bipolar derivations in precentral, opercular and insular cortices) showed extended and bilateral discharges in frontal lobes (mainly in opercular and precentral regions), with right predominance. EI analysis of five seizures was used to tailor the resection of the right opercular region with greater confidence than with standard clinical procedure. This patient is now seizure free with 2-year follow-up. Patient C was suffering from lesional partial epilepsy (mesial left occipital dysplatic lesion) with bilateral interictal abnormalities and contralateral ictal discharges (above right temporal region) on scalp EEG. SEEG recordings (90 bipolar derivations in occipital, parietal and temporal cortices and in hippocampus) showed lesional ictal onset with rapid spread to the fusiform gyri followed by bilateral discharges with right temporal lobe predominance. Two seizures were analysed with our methodology. This patient is now-seizure free with 1-year follow-up after resection limited to the occipital dysplastic region.

For a group study, we selected 10 MTLE patients in whom one spontaneous seizure was recorded, with the hippocampus being clinically identified as involved in the presumed SOZ. Those patients were included in a previous study on seizures induced by 1 Hz stimulation of temporal lobe structures (David *et al.* , 2008). Table 1 shows detailed information about patients, including suspected SOZ, with numbering of patients in accordance with (David *et al.* , 2008). For every patient, post-operative T1 anatomical MRI normalised in the MNI space was used to delineate the voxels that were either resected or disconnected from the rest of the brain.

Table 1 about here

II.3 Visual identification of the seizure onset zone

Each seizure was inspected visually to determine a baseline period and the SOZ, *i.e.* the exact timing of the first relevant electrical changes that occurred prior to the clinical onset of the seizure. The SOZ was defined from SEEG recordings using different patterns: (i) low-voltage fast activity over 20 Hz; (ii) recruiting fast discharge (around 10 Hz or more) of spikes or polyspikes; (iii) rhythmic activity (around 10Hz) of low amplitude. The origin of time for each seizure was determined from visual analyses just before suspected seizure onset. Baseline recordings were chosen as periods of at least 20 seconds without strong artefact or epileptic activity during the 5 minutes preceding each seizure.

II.4 Imaging of epileptogenicity

Figure 1 summarises the basic steps performed to obtain a statistical parametric map of epileptogenicity. Full details are provided in the following subsections.

Figure 1 about here

II.4.1 Preprocessing of SEEG signals

Based on previous research on focal epilepsies (Worrell *et al.* , 2004, Jirsch *et al.* , 2006, Bartolomei *et al.* , 2008), we assume here that the feature of interest for defining epileptogenicity of a brain region is the presence of rapid discharges, and that epileptogenic specificity of oscillations increases with frequency. Note however that this assumption can be relaxed in the proposed framework because any frequency band of interest can be chosen *a priori*. In particular, we will address below the impact of frequency selection on volume of activation and its correlation with resection and surgical outcome in our MTLE group data.

The presence of rapid discharges can be quantified after transformation of raw SEEG signals into the time-frequency plane around seizure onset, for instance using a Morlet Wavelet Transform (Le Van Quyen *et al.* , 2001), which gives as output for each electrode a measure of SEEG power $P(f,t)$, at time t and frequency f. We will consider this simple measure as the feature of interest to characterise epileptogenic activity.

Because of the lack of electrical homogeneity of the milieu that induces amplitude variations between electrodes, P needs to be normalised. It has been already proposed to normalise power in high frequencies ($12.4 \leq f < 97$ Hz) by power in low frequencies ($3.5 \leq f < 12.4$ Hz) to define the EI (Bartolomei *et al.* , 2008). Here, in agreement with (Worrell *et al.* , 2004), we choose to focus on high frequencies exclusively. This relaxes the assumption about a specific relationship between rapid discharges and slow waves. Therefore, mean power at seizure onset is compared to mean power obtained from a baseline recording of several seconds (typically between 20 and 60 seconds).

We propose that description of HFO bursts lasting a few seconds is sufficient to describe epileptogenic networks. Accordingly, we proceed as follows to extract SEEG features used to define the EI (Figure 1):

(i) The SEEG signal of each electrode is transformed into the time-frequency plane in time and frequency ranges relevant to the type of epilepsy under study. Here, for temporal and insular focal epilepsy, we used $\left[0 \quad 24\right]$ seconds and $\left[1 \quad 100\right]$ Hz with a temporal resolution dt of 100 ms and a spectral resolution df of 1 Hz.

(ii) To capture temporal changes of frequency distribution of power, overlapping epochs of data are successively selected from the time-frequency plane, whose duration D can be adapted to the expected duration of bursts of SEEG oscillations. In this study, we used $D = 4$ seconds. The onset Δ of each time window was taken from 0 to 20 seconds, with a time step $d\Delta$ of 2 seconds.

(iii) In principle, statistics of power at seizure onset can be obtained for every frequency (see below). However, in practice, one may want to focus on a

frequency band of interest where power is averaged over frequencies. We use [60 100] Hz in this study. The same frequency-specific averaging is performed on baseline data of duration D_b with the same time resolution dt between successive epochs.

II.4.2 Image transformation and statistics

At the end of SEEG processing, two distributions of power are thus obtained for each electrode and for each peri-onset time, with $\frac{D}{dt}$ samples during seizure and $\frac{D_b}{dt}$ samples during baseline. These data features are log transformed to render them more normally distributed (Kiebel *et al.* , 2005). In order to adopt a neuroimaging perspective, knowing SEEG electrode positions, SEEG log-power is interpolated in space on isotropic voxels of 4 mm width. Interpolation proceeds in two steps in order to obtain a good trade-off between anatomical precision and the extent of spatial sampling: (i) Nearest neighbour interpolation is performed in every voxel included in the volume defined by spheres of 5 mm radius centred on each electrode. It ensures that actual values of SEEG log-power will be attributed to voxels close to the electrodes. (ii) 3D linear interpolation is further performed in voxels located at a maximal distance of 10 mm from any electrode. Note that in the Matlab implementation of the linear interpolation that we used, the only voxels that can be considered are those that belong to the convex volume defined by the positions of electrodes.

Similarly to functional MRI, statistical analyses can then be performed in Statistical Parametric Mapping software (SPM8, Wellcome Department of Imaging Neuroscience, www.fil.ion.ucl.ac.uk/spm) on 3D images of log-power (Blauwblomme

et al. , In press). Statistics of the difference of log-power of rapid discharges between seizure and baseline are obtained using a standard two-sample t-test on the images of log-power (Kiebel *et al.* , 2005). Serial correlations in the data are taken into account by an autoregressive AR(1) model of noise covariance component, as used in fMRI time-series analysis (Friston *et al.* , 2002). Crucially, statistical parametric mapping allows one to control family-wise error (FWE) in the context of spatially correlated imaging data using the theory of Gaussian random fields (Friston *et al.* , 1996, Worsley *et al.* , 1996). Gaussian random field theory requires the data to be a good lattice approximation to continuous smooth Gaussian fields. We therefore smooth the log power images using an isotropic Gaussian kernel with a width of 3 millimetres (equivalent to the distance between successive electrodes).

II.4.3 Measures of epileptogenicity

For each peri-onset time Δ, we define the index of epileptogenicity as the t-value of the differences in smoothed log-power between seizure and baseline. Statistical significance is directly obtained with the associated p-value, FWE corrected. By applying a threshold on this p-value, it is possible to determine the regions showing significant rapid discharges for each peri-onset time Δ. In this study, we used $p<0.05$ FWE corrected. Furthermore, to obtain summarised information as to how seizures develop, we define a map of propagation delay of rapid discharges, showing for each voxel the minimal peri-onset time Δ for which this particular voxel was significantly activated.

II.4.4 Group analyses

Group analyses are important for two reasons: (i) to improve robustness of EI estimation when several seizures are recorded in a single subject; (ii) to highlight the most stable electrophysiological features observed in patients suffering from similar seizures and/or symptoms.

When several seizures are recorded in the same patient on the same electrodes, corresponding data can be pooled together to perform a fixed-effect statistical analysis, under the assumption that the same process has been recorded several times (Friston *et al.* , 1999). The epileptogenicity index and the propagation delay are then obtained using the same procedure as when a single seizure is analysed. In rare cases where a large number of seizures are recorded (typically more than 10), a random-effect statistical analysis might be preferred, where the values of EI are entered into a one-sample t-test as a second-level analysis (Friston *et al.* , 1999).

For group studies of patients suffering from the same type of seizure, random-effect second level analyses could also be performed, provided the size of the group is sufficiently large. To do so, the brains need to be normalised in the same anatomical space, typically the MNI coordinates in SPM8 (Ashburner, 2009), as is classically done in neuroimaging studies. However, because the brain is not identically sampled between patients, all images of EI do not share exactly the same voxels: some voxels might be sampled in many patients, *e.g.* the hippocampus in MTLE, whereas others might not be. As a solution to this caveat, we propose to perform conjunction analyses in order to obtain images encoding the group probability of finding a significant EI for each voxel. It proceeds in three steps:

(i) Define a common space for all patients. It is done by selecting voxels recorded in a large proportion of patients, in order to get a sufficient amount of data for robust estimation of the EI group distribution. For this study, we used voxels recorded in at least 50% of patients.

(ii) For every patient, obtain a binary map showing voxels having a significant EI. We used p<0.05 FWE corrected in this study. Those maps are inclusively masked with the common space to retain only those voxels that have been repetitively explored.

(iii) The *group probability map of EI* is obtained by averaging together subject-level binary maps of EI.

The values of the group probability map range between 1 (voxels systematically showing significant EI values when recorded) and 0 (voxels found to never show significant EI when recorded). Those maps are obtained for every values of peri-onset time Δ. Finally, a *group propagation delay map* can be defined, which encodes the minimum peri-onset time Δ for which the group probability map is above a threshold q. In other words, if $q = 0.5$, the group propagation delay map shows the time after seizure onset needed to record rapid discharges in half of the patients. The threshold q was set to 0.5 for this study.

As an alternative to this probabilistic procedure for group studies, it is always possible to perform ROI-based non parametric tests as performed in (Worrell *et al.* , 2004, Bartolomei *et al.* , 2010, Bartolomei *et al.* , 2011, Vaugier *et al.* , 2009, Aubert *et al.* , 2009). This will not be considered in this study.

II.4.5 Software implementation

Methods were implemented in a SPM8 toolbox dedicated to the analysis of intracerebral EEG that is developed in-house (O.D.). It is based on standard routines of SPM8 for spatial processing of MRI, EEG analysis and statistics.

III RESULTS

III.1 Patient A

Two reflex seizures to strawberry syrup consumption were recorded, which started with loss of consciousness, followed by facial flushing, oro-alimentary automatisms, repeated swallowing and sialorhea, and ended with postictal confusion and amnesia. From visual analysis of SEEG (Figure 2), seizures start in the anterior inferior portion of the insula with a high amplitude spike followed by a low voltage high frequency discharge with secondary spreading to the hippocampus and then to the frontal and temporal neocortex. Both seizures look remarkably similar, as can be expected from reflex seizures.

The insular area explored by the tip of electrode Y (middle short gyrus of the insula), showing the earliest fast discharges, was resected (Blauwblomme *et al.* , In press) and the patient is now seizure free after 3 year follow-up. It defines this region as the epileptogenic zone.

Time-frequency charts of $P(f,t)$ can be normalised by the baseline by subtracting the baseline mean and by dividing by the baseline standard deviation for each frequency for convenient visualisation of SEEG features of interest to define the EI. For Seizure 1, they show (Figure 3): (i) rapid discharges (>15 Hz) and slow waves (<15 Hz) are modulated differently in time; (ii) seizure onset zone (Y) is characterised by early rapid discharges; (iii) rapid discharges show different frequency distribution between brain regions and across time for the same region with a timescale of a few seconds (~5 seconds); (iv) seizure onset zone (Y) show more rapid discharges than those in other regions.

Figures 2 & 3 about here

In agreement with Figure 3, EI mapping at seizure onset ($\Delta = 0$ s) identified the seizure focus at the tip of electrode Y in the middle portion of the insula (Figure 4A). Furthermore, EI maps of Seizure 1 and Seizure 2 analysed both separately, and together with a fixed effect, shows a very good reproducibility of EI maps between seizures (Figure 4B). It also indicates how rapid discharges propagate over time, as also shown in time-frequency charts of Figure 3. This type of information is summarised in the map of seizure propagation delay (Figure 4C), which shows an early involvement of the middle inferior insula ($\Delta = 0$ s), followed by the activation of the posterior temporal cortex ($\Delta = 7$ s), of the hippocampus ($\Delta = 10$ s) and of the prefrontal lateral cortex and anterior superior insula ($\Delta = 18$ s).

Figure 4 about here

III.2 Patient B and Patient C

In both patients, bilateral electrode implantation (Figure 5, top left) was used because SOZ lateralisation could not be determined without SEEG recordings: EEG abnormalities were diffused without any associated brain lesion in Patient B and seizures on scalp EEG were lateralised on the right side although a left occipital dysplastic lesion could be observed on the MRI.

In Patient B, epileptogenicity maps were obtained on 5 seizures using a fixed-effect analysis. They clearly confirmed the bilateral involvement of opercular regions and of right precentral regions (see SEEG recordings of Seizure 1, Figure 5 bottom right). The seizure propagation map contained only zeroes (Figure 5, right), indicating very fast onset in all implanted regions. However, the epileptogenicity index at seizure onset ($\Delta = 0$ s) was the largest in the right opercular region (Figure 5, bottom left), which was finally successfully resected (Figure 5, top right).

The two seizures recorded during SEEG in Patient C confirmed that HFOs originated from the dysplastic lesion before propagating to bilateral temporal regions (see SEEG recordings of Seizure 1, Figure 5 bottom right). Epileptogenicity maps (fixed effect analysis of both seizures) were highly successful in reconstructing HFO propagation, with significant EI restricted to the dysplastic lesion at seizure onset ($\Delta = 0$ s) and propagation delay map showing a gradient of activation from mesial towards lateral regions, with late activation of the hippocampus (Figure 5). Such information allowed the successful resection of the dysplastic lesion in left occipital region (Figure 5, top right).

Figure 5 about here

III.3 Group study

Figure 6 shows SEEG recordings obtained in the hippocampus for all patients, using channels associated with the largest hippocampal EI at peri-onset time $\Delta = 0$ s. From a standard visual analysis of those recordings, electroclinical signatures clearly differed between patients, though they all involve the hippocampus to some extent. Therefore we considered that this dataset was interesting, with well-balanced reproducibility and heterogeneity, for a first demonstration of the robustness of the proposed methodology for seizure onset mapping in the context of group studies (Figure 7).

Despite inter-individual variability of SEEG recordings, EI maps ($p<0.05$ FWE corrected) at seizure onset clearly highlight regions of the temporal lobe, and particularly the hippocampus, in all patients (Figure 7A). Group probability maps of EI (Figure 7B) point towards the hippocampus as a strong generator of rapid discharges. They also indicate that the propagation of rapid discharges from hippocampus towards the temporal neocortex and the insula is a common feature in all subjects. This dynamical information is summarised in the group propagation delay map (Figure 7C), which shows the early involvement ($\Delta = 0$ s) of the hippocampus. The three-dimensional exploration of this map (not shown) indicates the following order of activation: hippocampus ($\Delta = 0$ s), temporal pole ($\Delta = 5$ s),

anterior inferior insula ($\Delta = 5$ s), posterior inferior insula ($\Delta = 9$ s), frontal operculum ($\Delta = 9$ s), temporal neocortex T2 ($\Delta = 14$ s).

Figures 6 & 7 about here

In addition, we evaluated the specificity of the epileptogenicity index in identifying the SOZ as a function of frequency, from 2 to 100 Hz. To do so, statistical maps of EI were computed for every frequency and thresholded at $p<0.05$, FWE corrected. Binary maps of EI were then compared to resected or disconnected parts of the temporal lobe in every patient by computing the overlap between the two maps (ratio of activated voxels included in the resection/disconnection mask). The activation size was also calculated and defined as the number of activated voxels divided by the number of voxels included in the resection/disconnection mask. Figure 8 shows those two quantities arranged according to Engel's classification of patients (IA n=7, median value reported in the Figure; IIIA n=1; IIB n=1; IIC n=1). Interestingly for all patients, the activation size decreased with frequencies, indicating that more focal activations are obtained when focusing on fast oscillations. A dissociation seemed to emerge between the group of IA patients and other isolated patients because IA patients showed a median activation size well below that of the other three patients, for frequencies higher than 20 Hz. Overlap index increased with frequencies in all patients, indicating that HFOs were more restricted to resected parts than other types of oscillations. Though median overlap of patients IA was excellent in HFOs (~80%), it could not be used to classify patients (Patients IIIA and IIB at ~50 % but Patient IIC at 90%).

Figure 8 about here

IV DISCUSSION

We proposed in this study a neuroimaging approach to the mapping of the SOZ, and of networks of propagation, that is based on the quantification of fast oscillations recorded in implanted epileptic patients. Obviously, observed statistical effects can be obtained only in regions that are actually explored with intracranial electrodes. Spatial sampling of images is thus limited to some parts of the brain, and inferences about epileptic networks provided by this technique may provide only a truncated version of the full picture. However, we showed that our procedure was very helpful to perform accurate and quantified identification of the SOZ in three patients who were seizure-free after tailored resection of regions with highest EI at seizure onset. In addition, we demonstrated in Patient A very good reproducibility of epileptogenicity mapping between two reflex seizures. Our procedure can also be used to perform group studies, as shown in a group of MTLE patients. It constitutes an important step forward in comparison to other approaches (Worrell *et al.* , 2004, Bartolomei *et al.* , 2008, Gnatkovsky *et al.* , 2011) for two main reasons that are discussed below.

Methodologically, the main advantage of the neuroimaging approach is to use the convenient and well-known statistical framework of SPM. In particular, SPM allows for correction of multiple comparisons by controlling the FWE rate, assuming that images are smooth. Though SEEG signals may record very focal dynamic signatures, the main features of SEEG signals are often relatively stable within the

same structure, thereby allowing a degree of smoothness of images compatible with statistical assumptions of SPM. Therefore, we have redefined the index of epileptogenicity to conform to Gaussian statistics in order to have access, with its p-value, to the significance of this index for a particular structure and patient, without referring to relative values as in (Bartolomei *et al.* , 2008, Gnatkovsky *et al.* , 2011). In addition, we have explicitly separated spectral and temporal information using the frequency-specific modulation of power in time as unique feature of interest. This allows to reconstruct, from statistical maps of EI obtained over peri-onset time, the slow propagation of fast oscillations, from the seizure onset zone towards the rest of the epileptogenic network. Last but not least, by the means of standardisation of patients' brains in the MNI space, group analyses become straightforward to perform. Our framework thus is a very powerful way to conduct the analysis of large series of patients. In particular, conjunction analyses provide probabilities of recording HFOs at seizure onset in every region of the brain that has been systematically recorded in a given type of seizure. It therefore provides important information on the physiopathology of epilepsies. More pragmatically, one could also envisage using those maps to optimise SEEG implantation procedures in similar cases by preferentially targeting those regions with the highest probability of producing HFOs at seizure onset. In another perspective, the method should also be useful to better understand the cortical networks underlying ictal clinical signs and symptoms that are common to a group of patients, but do not necessarily occur at the same time, nor in the same type of epilepsy. In other words, it can be used to decompose neural networks of seizure semiology.

On a clinical standpoint, our approach is very interesting because, once the origin of peri-onset time has been positioned and the baseline selected, epileptogenicity maps are obtained automatically and quickly. They easily provide maps summarising, and quantifying in a statistical framework, very complex signals that are sometimes difficult to analyse visually. It is very easy to navigate through maps of epileptogenicity and to adjust the significance level if necessary. Cross-validation of computational and visual analysis of SEEG signals is obviously mandatory, but our approach largely improves the spatial representation of the epileptogenic network of patients that are candidate for resective surgery. In other words, it provides objective data quantification in addition to clinical standard procedures that are powerful but remain subjective. In addition, using a data format compatible with most neuroimaging software, SEEG maps can be superimposed on other neuroimaging modalities in the same neuroanatomical space for multimodal exploration of epilepsies, e.g. see (Blauwblomme *et al.* , In press).

Here, we have illustrated the clinical interest of our approach to SOZ mapping in a patient having reflex epilepsy to syrup consumption. This patient was chosen due to being already fully documented with multimodal exploration (Blauwblomme *et al.* , In press). Interestingly, the SOZ was robustly estimated with the automatic procedure in a position that matched exactly with the successful resection of the middle short gyrus of the insula. Furthermore, the propagation of fast discharges within an insular-temporal network was evidenced. This is reminiscent with the temporal semiology of seizures. Two other patients suffering from cryptogenic frontal epilepsy and from lesional occipital epilepsy were also used to further demonstrate that very specific mapping of the SOZ and of propagation pathways can be achieved on a single

subject basis for clinical use. In addition, we have performed a group study of MTLE patients on a relatively small scale (10 patients) as a proof of concept. Though the numbers of patients included here was limited, it is clear that robust estimation of the SOZ was obtained, with spatial variability reflecting differences of SEEG recordings between patients. The group analysis clearly identified the hippocampus as being the SOZ, and in addition it was possible to describe a mean propagation pathway of fast discharges originating in the hippocampus. Interestingly, both the temporal pole and the insular cortex were shown to be quickly involved, as suggested in other SEEG studies where analyses were done visually (Chabardes *et al.* , 2005, Isnard *et al.* , 2000). Nonetheless, a significant variability was observed in individual maps of EI (Figure 6) because of important differences in electroclinical signatures of seizures. The hippocampal-insular-polar network is thus a key network in MTLE epilepsy in this population of patients, but further refinements can in principle be obtained in its description by conducting larger clinical studies with less heterogeneous patients.

Another reason that we presented our group study was to demonstrate that there are particular data features that have greater predictive validity in relation to prognosis following surgical intervention. In particular, we were able to interrogate the data by looking for systematic increases in power during seizure onset activity over different frequencies. We were then able to compare the results at different frequencies with the areas removed surgically in a region-specific manner and interpret these in terms of clinical outcome. This sort of analysis is very important and can only be pursued at the between-subject level, to validate the particular data features employed at the within-subject level. Though the group studied here is too small to reach a definitive conclusion, our results confirmed that fast oscillations were more likely than slow

oscillations to indicate the SOZ, and therefore to represent a good electrophysiological marker of the surgical target, mainly because they were more focal, in particular in patients with best outcome.

The main prior of the proposed approach is the knowledge of the frequency band of interest. Here we presented results obtained with a focus on high gamma range (60-100 Hz), which is known to be typically involved in temporal and insulo-temporal seizures (Bartolomei *et al.* , 2008, Bartolomei *et al.* , 2010). When comparing EI distribution over frequencies (Figure 8), it is evident that one had to choose the highest frequencies to be the most specific and that the choice of 60-100 Hz was a good one in this dataset. However it remains unclear whether HFOs are a good marker of epileptogenic networks in every type of epilepsy. It will have to be tested in future studies, and the framework proposed here will allow to do so.

Overall, our findings suggest that, in addition to providing keys to SOZ identification and seizure propagation, the proposed methodology is likely to be used for diagnostic purposes and might thus help improve patient outcome. These issues will be further clarified in future studies.

ACKNOWLEDGEMENTS

We thank Elena Ryapolova, UCSF, for a critical reading of the manuscript. This work was supported by ANR (project MLA, number ANR-2010-BLAN-1409-02).

FIGURE CAPTIONS

Figure 1:

Summary of the procedure to obtain a map of EI at peri-onset time Δ and in a frequency band f, from SEEG signals and electrode positions.

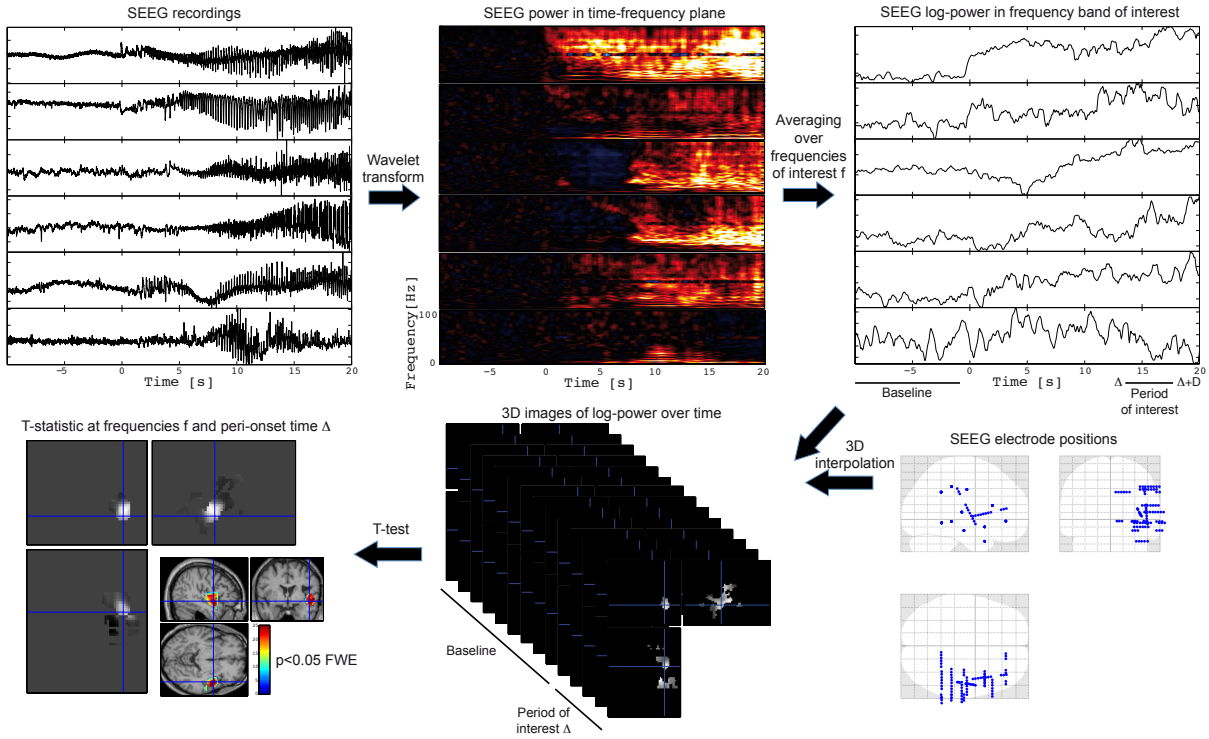

Figure 2:

Top: Coronal (left) and lateral (right) representation of the stereotaxic implantation scheme. Bottom: SEEG recordings of two reflex seizures to strawberry syrup intake showing ictal onset in the right anterior inferior insula (Y) and secondary spreading in the hippocampus (B-C). Y: anterior inferior insula; X: anterior superior insula; C: posterior hippocampus; B: anterior hippocampus; I: temporal pole; S: dorsolateral anterior parietal cortex.

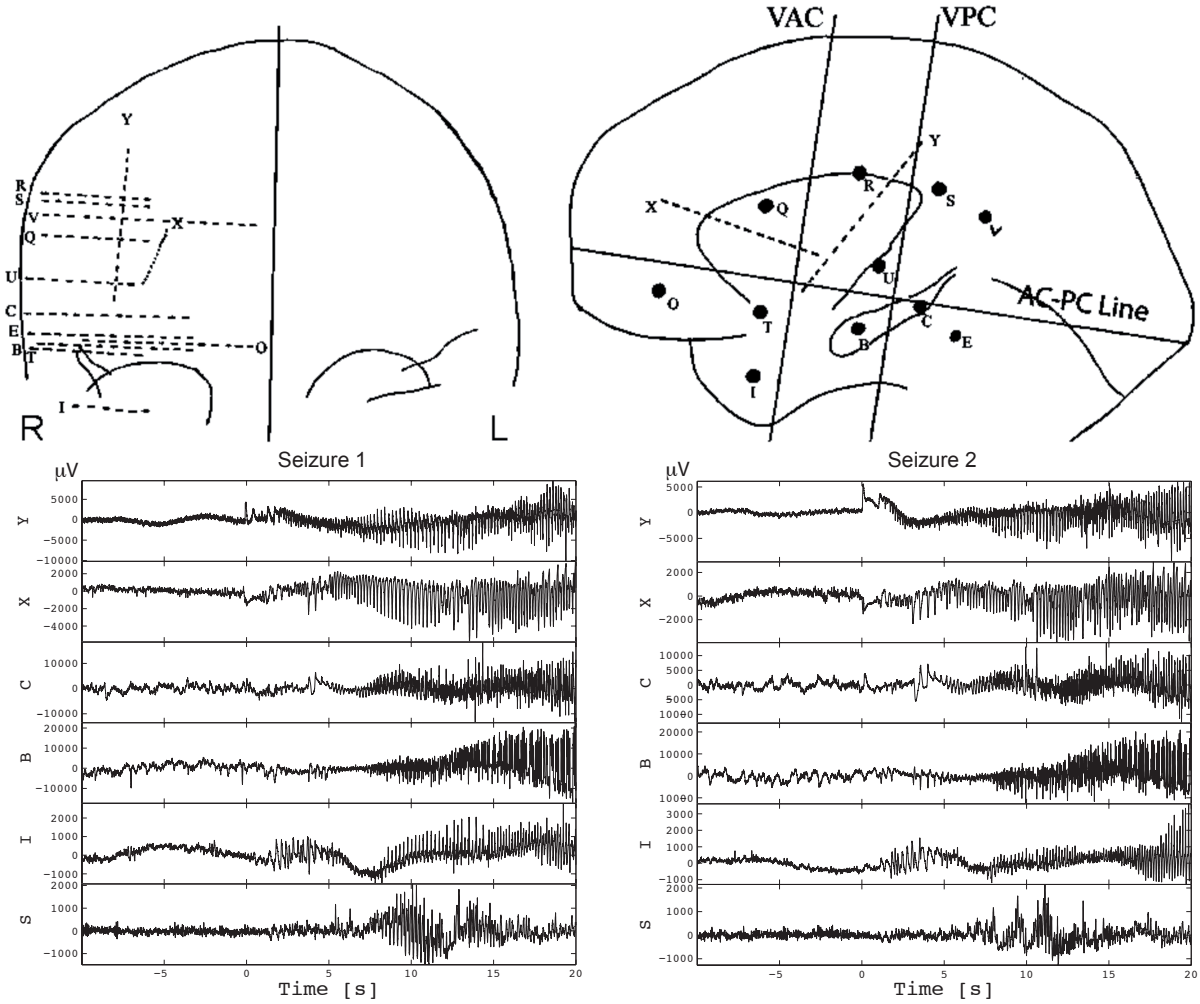

Figure 3:

Time-frequency chart of normalised power of Seizure 1 (Figure 2). Colour codes for standard deviation of power according to baseline. Vertical bar indicates seizure onset.

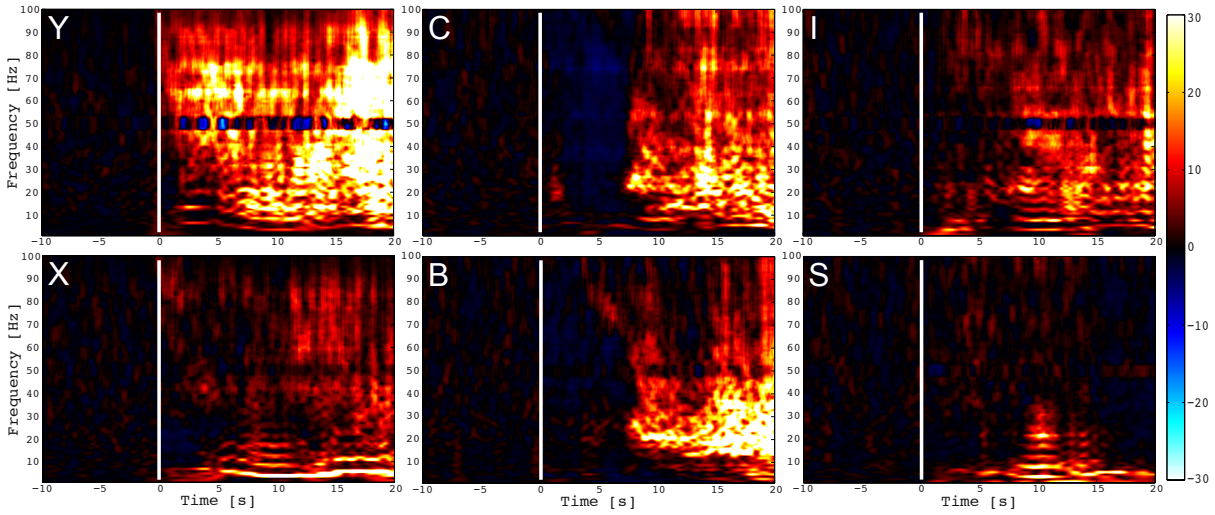

Figure 4:

Epileptogenicity mapping of a case of reflex insular epilepsy. A. Map of significant (p<0.05 FWE corrected) epileptogenicity index obtained at $\Delta = 0$ s, with a fixed effect analysis of the two recorded seizures. Blue dots indicate actual recording sites. B. Maps of significant (p<0.05 FWE corrected) epileptogenicity index obtained at different peri-onset time ($\Delta = 0$ s; $\Delta = 10$ s; $\Delta = 20$ s), each seizure analysed separately or together using a first level fixed effect analysis. Red indicates the most significant EI. C. Map of seizure propagation delay in seconds, estimated from the fixed effect analysis of the two recorded seizures. Blue indicates the lowest propagation delay, i.e. the SOZ.

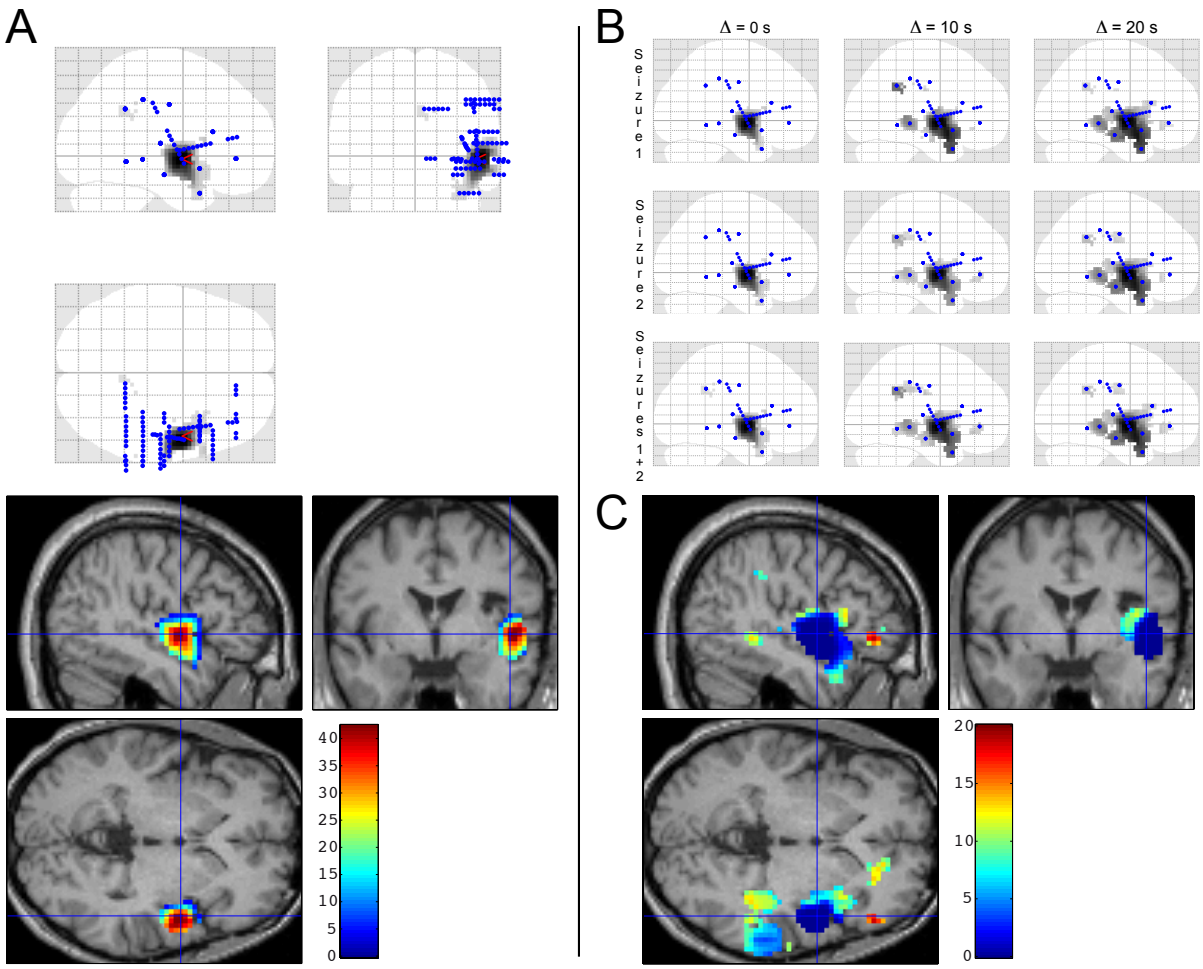

Figure 5:

Epileptogenicity mapping of cryptogenic frontal epilepsy (Patient B) and of lesional occipital epilepsy (Patient C). Left: Map of significant (p<0.05 FWE corrected) epileptogenicity index obtained at $\Delta = 0$ s, with a fixed effect analysis of recorded seizures (Patient B: n=5; Patient C: n=2). Top right: T1 MRI showing resection actually performed (red rectangle). Middle right: Map of seizure propagation delay in seconds, estimated from the fixed effect analysis of all recorded seizures. Bottom right: SEEG recordings of a seizure in regions shown with numbers in MRI. Asterisks indicate latency of detection of first significant HFOs.

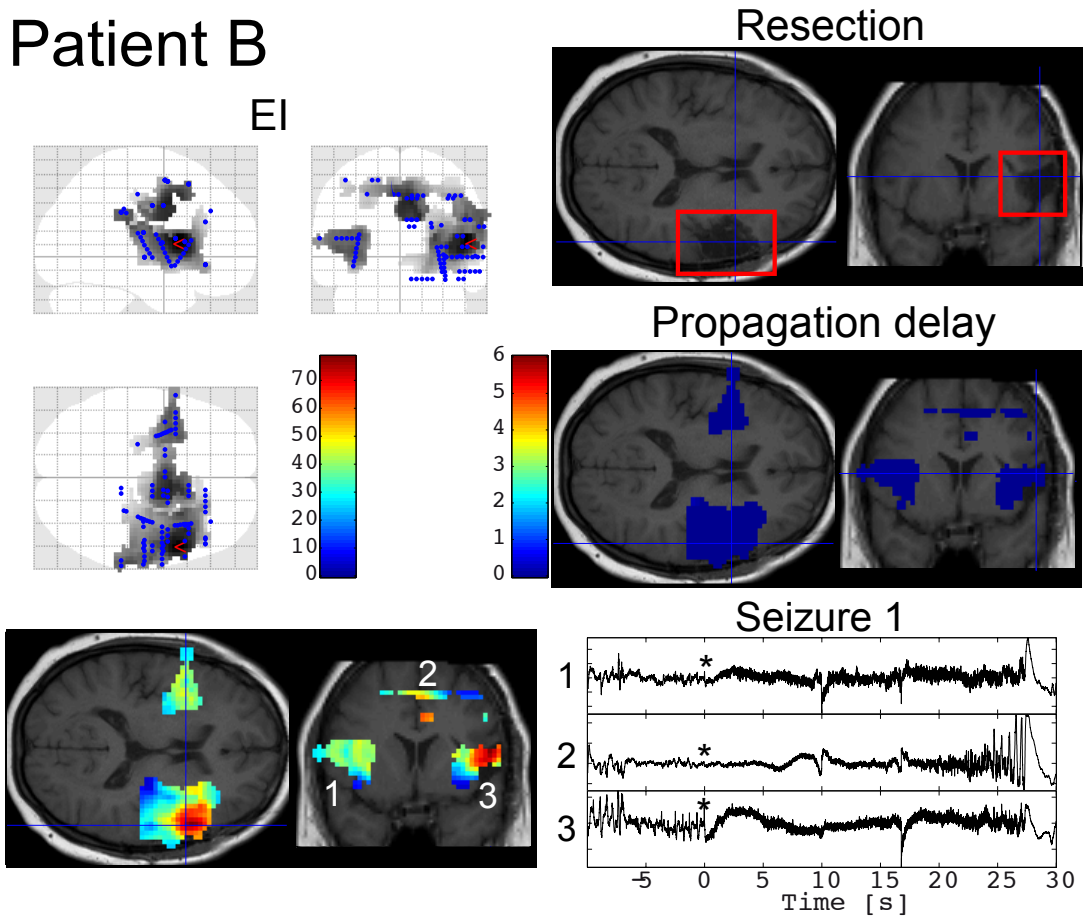
Patient B
Resection
EI
Propagation delay
70
60
50
40
30
20
10
0
6
5
4
3
2
1
0
Seizure 1
1
2
3
-5
0
5
10
15
20
25
30
Time [s]

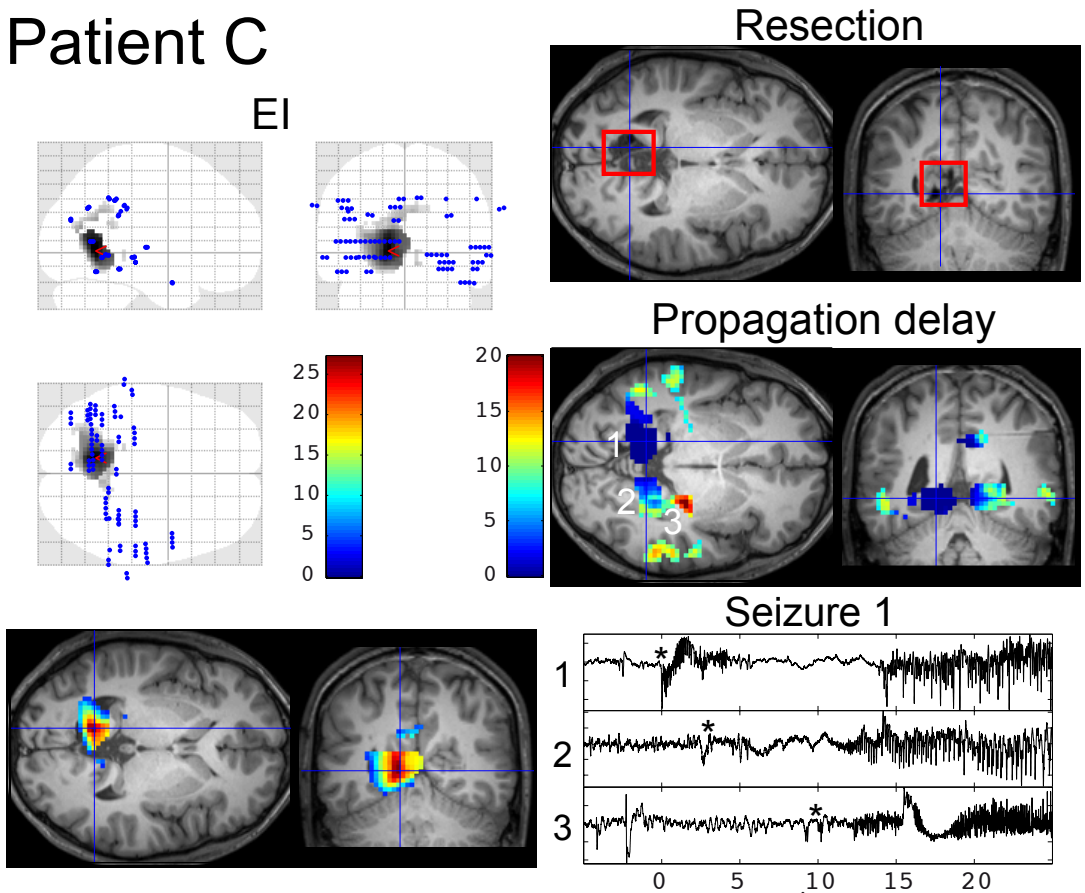
Patient C
Resection
EI
Propagation delay
25
20
15
10
5
0
20
15
10
5
0
Seizure 1
1
2
3
0
5
10
15
20
Time [s]

Figure 6:

Hippocampus activity at seizure onset of every patient. Numbers on the left hand side indicate EI values at peri-onset time $\Delta = 0$ s.

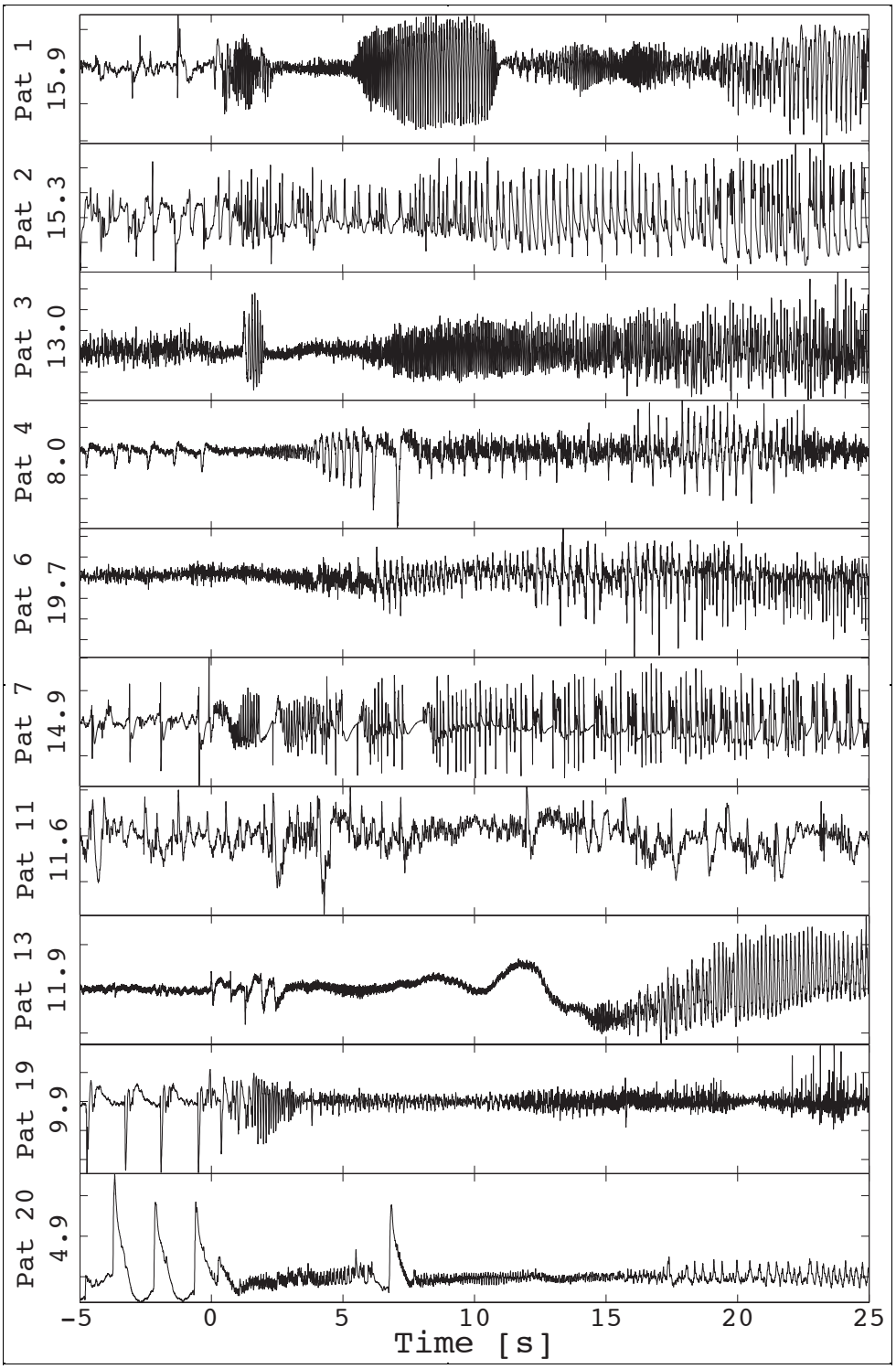

Figure 7:

Group mapping of epileptogenicity of mesio-temporal lobe epilepsy. A. Map of significant (p<0.05 FWE corrected) epileptogenicity index obtained at $\Delta = 0$ s in the ten patients. B. Group probability maps of EI (p<0.05 FWE corrected) obtained at different peri-onset times ($\Delta = 0$ s; $\Delta = 10$ s; $\Delta = 20$ s). Blue dots show recording sites obtained in all patients. C. Group map of seizure propagation delay in seconds.

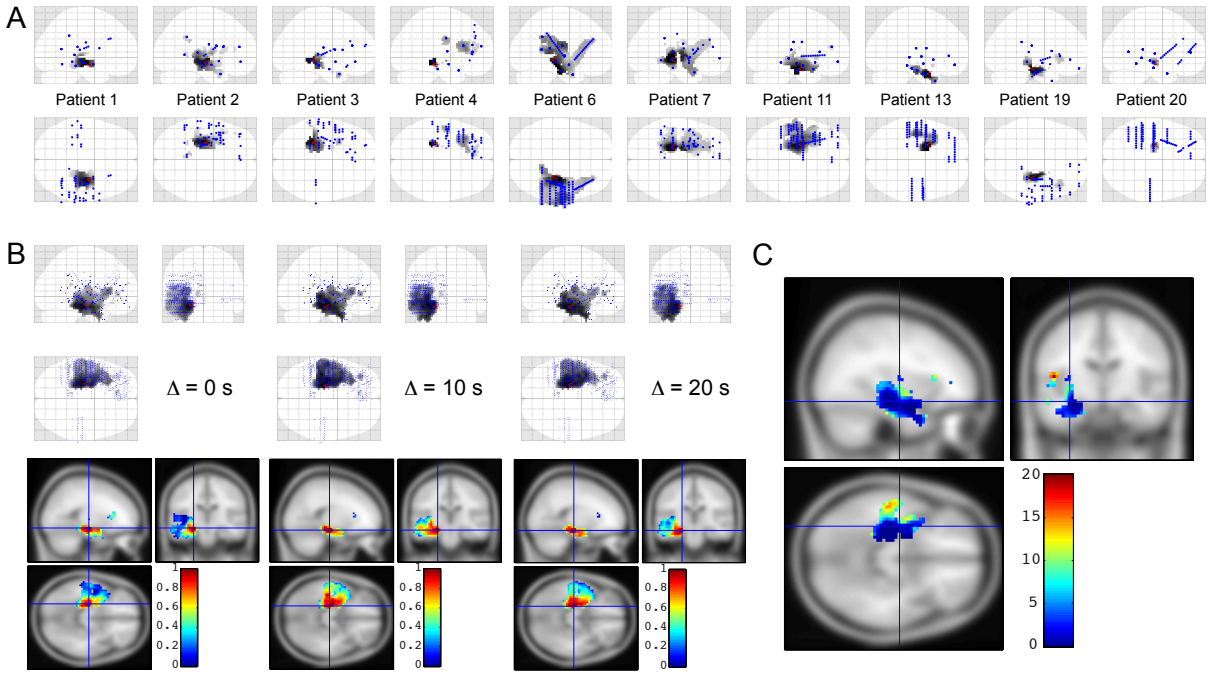

Figure 8: Correlation between frequency-specific EI maps, surgical intervention and post-surgical outcome. See text for details.

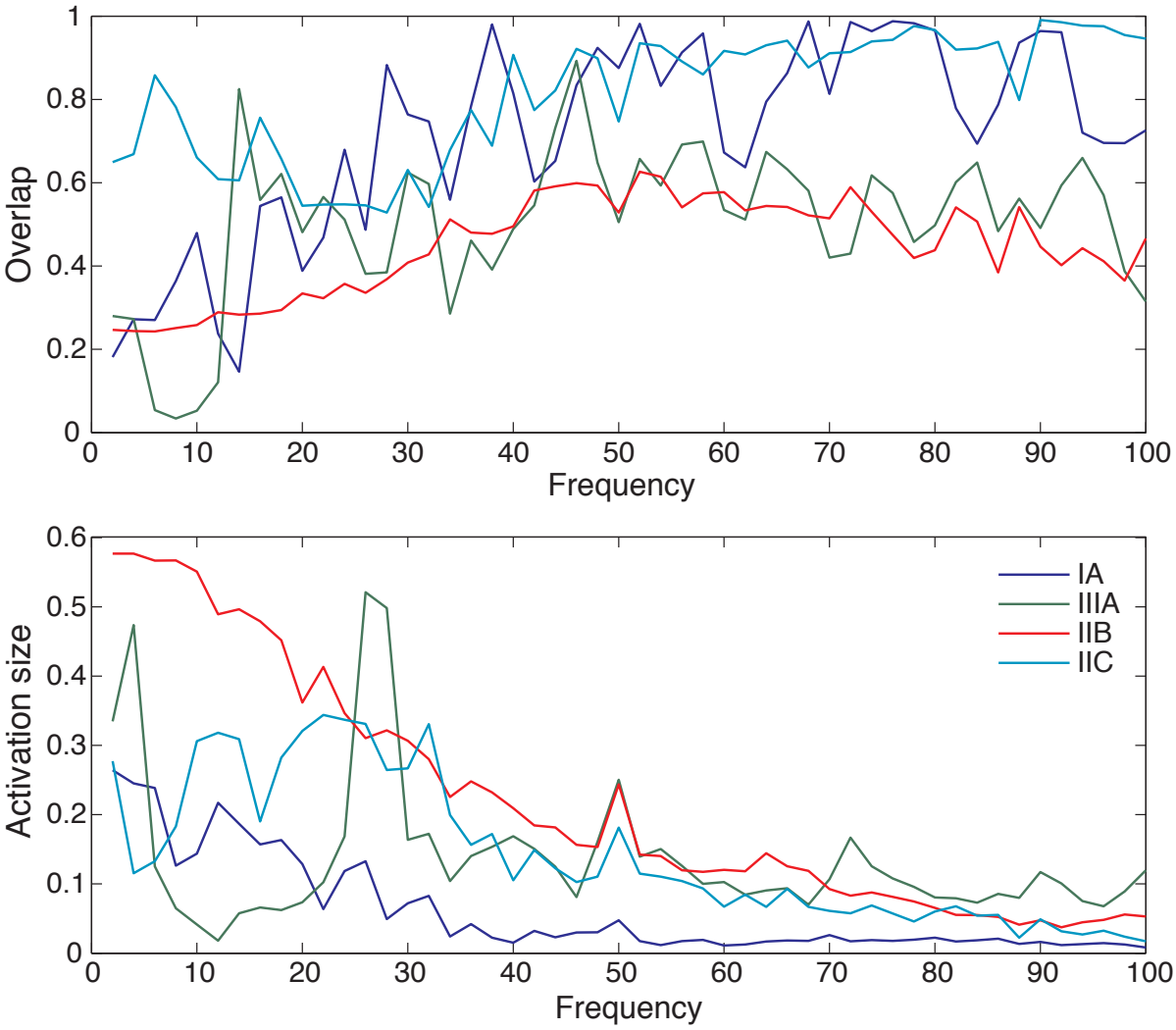
Overlap
Frequency
Activation size
Frequency
IA
IIIA
IIB
IIC

REFERENCES

Alarcon G, Binnie CD, Elwes RD, Polkey CE. Power spectrum and intracranial EEG patterns at seizure onset in partial epilepsy. Electroencephalogr Clin Neurophysiol. 1995 May;94(5):326-37.

Allen PJ, Fish DR, Smith SJ. Very high-frequency rhythmic activity during SEEG suppression in frontal lobe epilepsy. ElectroencephalogrClinNeurophysiol. 1992;82(2):155-9.

Ashburner J. Computational anatomy with the SPM software. Magn Reson Imaging. 2009 Oct;27(8):1163-74.

Aubert S, Wendling F, Regis J, McGonigal A, Figarella-Branger D, Peragut JC, et al. Local and remote epileptogenicity in focal cortical dysplasias and neurodevelopmental tumours. Brain. 2009 Nov;132(Pt 11):3072-86.

Bancaud J, Angelergues R, Bernouilli C, Bonis A, Bordas-Ferrer M, Bresson M, et al. Functional stereotaxic exploration (SEEG) of epilepsy. Electroencephalogr Clin Neurophysiol. 1970 Jan;28(1):85-6.

Bartolomei F, Chauvel P, Wendling F. Epileptogenicity of brain structures in human temporal lobe epilepsy: a quantified study from intracerebral EEG. Brain. 2008 Jul;131(Pt 7):1818-30.

Bartolomei F, Cosandier-Rimele D, McGonigal A, Aubert S, Regis J, Gavaret M, et al. From mesial temporal lobe to temporoperisylvian seizures: a quantified study of temporal lobe seizure networks. Epilepsia. 2010 Oct;51(10):2147-58.

Bartolomei F, Gavaret M, Hewett R, Valton L, Aubert S, Regis J, et al. Neural networks underlying parietal lobe seizures: A quantified study from intracerebral recordings. Epilepsy Res. 2011 Feb;93(2-3):164-76.

Blauwblomme T, Kahane P, Minotti L, Grouiller F, Krainik A, Hoffman D, et al. Multimodal imaging of physiological and pathological gamma activity in a case of eating reflex seizure. J Neurol Neurosurg Psychiatry. In press.

Chabardes S, Kahane P, Minotti L, Tassi L, Grand S, Hoffmann D, et al. The temporopolar cortex plays a pivotal role in temporal lobe seizures. Brain. 2005;128(Pt 8):1818-31.

David O, Wozniak A, Minotti L, Kahane P. Preictal short-term plasticity induced by intracerebral 1 Hz stimulation. Neuroimage. 2008;39(4):1633-46.

Fisher RS, Webber WR, Lesser RP, Arroyo S, Uematsu S. High-frequency EEG activity at the start of seizures. JClinNeurophysiol. 1992;9(3):441-8.

Friston KJ, Holmes A, Poline JB, Price CJ, Frith CD. Detecting activations in PET and fMRI: levels of inference and power. Neuroimage. 1996 Dec;4(3 Pt 1):223-35.

Friston KJ, Holmes AP, Worsley KJ. How many subjects constitute a study? Neuroimage. 1999;10(1):1-5.

Friston KJ, Penny W, Phillips C, Kiebel S, Hinton G, Ashburner J. Classical and Bayesian inference in neuroimaging: theory. Neuroimage. 2002;16(2):465-83.

Gnatkovsky V, Francione S, Cardinale F, Mai R, Tassi L, Lo Russo G, et al. Identification of reproducible ictal patterns based on quantified frequency analysis of intracranial EEG signals. Epilepsia. 2011 Mar;52(3):477-88.

Grenier F, Timofeev I, Steriade M. Neocortical very fast oscillations (ripples, 80-200 Hz) during seizures: intracellular correlates. JNeurophysiol. 2003;89(2):841-52.

Isnard J, Guenot M, Ostrowsky K, Sindou M, Mauguiere F. The role of the insular cortex in temporal lobe epilepsy. Ann Neurol. 2000 Oct;48(4):614-23.

Jirsch JD, Urrestarazu E, LeVan P, Olivier A, Dubeau F, Gotman J. High-frequency oscillations during human focal seizures. Brain. 2006;129(Pt 6):1593-608.

Kiebel SJ, Tallon-Baudry C, Friston KJ. Parametric analysis of oscillatory activity as measured with EEG/MEG. HumBrain Mapp. 2005;26(3):170-7.

Le Van Quyen M, Foucher J, Lachaux J, Rodriguez E, Lutz A, Martinerie J, et al. Comparison of Hilbert transform and wavelet methods for the analysis of neuronal synchrony. JNeurosci Methods. 2001;111(2):83-98.

Rosenow F, Luders H. Presurgical evaluation of epilepsy. Brain. 2001;124(Pt 9):1683-700.

Spencer SS, Sperling MR, Shewmon DA, Kahane P. Intracranial electrodes. In: Engel J, Jr., Pedley TA, editors. Epilepsy: A Comprehensive Textbook. Philadelphia: Lippincott Williams & Wilkins; 2008. p. 1791-815.

Tellez-Zenteno JF, Dhar R, Wiebe S. Long-term seizure outcomes following epilepsy surgery: a systematic review and meta-analysis. Brain. 2005 May;128(Pt 5):1188-98.

Vaugier L, Aubert S, McGonigal A, Trebuchon A, Guye M, Gavaret M, et al. Neural networks underlying hyperkinetic seizures of "temporal lobe" origin. Epilepsy Res. 2009 Oct;86(2-3):200-8.

Wendling F, Bartolomei F, Bellanger JJ, Bourien J, Chauvel P. Epileptic fast intracerebral EEG activity: evidence for spatial decorrelation at seizure onset. Brain. 2003;126(Pt 6):1449-59.

Worrell GA, Parish L, Cranstoun SD, Jonas R, Baltuch G, Litt B. High-frequency oscillations and seizure generation in neocortical epilepsy. Brain. 2004;127(Pt 7):1496-506.

Worsley KJ, Marrett S, Neelin P, Vandal AC, Friston KJ, Evans AC. A unified statistical approach for determining significant signals in images of cerebral activation. Hum Brain Mapp. 1996;4(1):58-73.